RESEARCH ARTICLE

Role of acidic sphingomyelinase in thymol-mediated dendritic cell death

Nguyen Thi Xuan[1], Ekaterina Shumilina[1], Evi Schmid[1], Shefalee K. Bhavsar[1], Rexhep Rexhepaj[1], Friedrich Götz[2], Erich Gulbins[3] and Florian Lang[1]

[1] Department of Physiology, University of Tübingen, Tübingen, Germany
[2] Department of Physiology, Microbial Genetics, University of Tübingen, Tübingen, Germany
[3] Institute of Molecular Biology, University of Duisburg-Essen, Essen, Germany

Scope: Thymol is a component of several plants with antimicrobial activity. Little is known about the effects of thymol on immune cells of the host. This study addressed the effects of thymol on dendritic cells (DCs), regulators of innate and adaptive immunity.
Methods and results: Immunohistochemistry, Western blotting and fluorescence-activated cell sorting analysis were performed in bone marrow-derived DCs either from wild-type mice or from mice lacking acid sphingomyelinase ($ASM^{-/-}$) treated and untreated for 24 h with thymol (2–100 μg/mL). Thymol treatment resulted in activation of ASM, stimulation of ceramide formation, downregulation of anti-apoptotic Bcl-2 and Bcl-xL proteins, activation of caspase 3 and caspase 8, DNA fragmentation as well as cell membrane scrambling. The effects were dependent on the presence of ASM and were lacking in $ASM^{-/-}$ mice or in wild-type DCs treated with sphingomyelinase inhibitor amitriptyline.
Conclusion: Thymol triggers suicidal DC death, an effect mediated by and requiring activation of ASM.

Received: November 30, 2009
Revised: May 17, 2010
Accepted: May 23, 2010

Keywords:
Cytokines / LPS / Maturation / Phosphatidylserine

1 Introduction

Thymol is well known for its antibacterial [1, 2] and antifungal [3] potency. Little is known, however, about its effect on the host immune system. It has been shown to influence the generation of reactive oxygen species [4] and, at higher concentrations, to induce DNA damage [5] and to inhibit cell proliferation [6]. In erythrocytes, it protects against suicidal cell death [7].

This study analyzed the effect of thymol on the survival and function of dendritic cells (DCs). On the one hand, DCs play a critical role in the initiation of immune responses to pathogens [8–10]. On the other hand, they also prevent potentially damaging immune responses being directed against a multitude of harmless antigens to which the body is exposed daily. These roles are particularly important in the intestine, where only a single layer of epithelial cells provides a barrier against billions of commensal microorganisms, pathogens and food antigens, covering a large surface area. In the intestine, therefore, a key requirement of DCs is to generate oral tolerance to food antigens, while preserving immunity to pathogens [11, 12]. DCs are in close contact with the intestinal epithelium [12]. Epithelial Toll-like receptor engagement provokes DCs to extend processes into the intestinal lumen for direct bacterial uptake [13].

This study shows that thymol stimulates apoptotic death of DCs and addresses the underlying mechanisms.

Correspondence: Professor Florian Lang, Physiologisches Institut der Universität Tübingen, Gmelinstrasse 5, D-72076 Tübingen, Germany
E-mail: florian.lang@uni-tuebingen.de
Fax: +49-7071-29-5618

Abbreviations: ASM, acid sphingomyelinase; **AWB,** annexin washing buffer; **DAG,** 1,2-diacylglycerol; **DC,** dendritic cell; **FACS,** fluorescence-activated cell sorting; **FCS,** fetal calf serum; **siRNA,** small interfering RNA

2 Materials and methods

2.1 Cell culture

DCs were obtained from bone marrow of 7 to 12 wk-old acid sphingomyelinase ($ASM^{-/-}$) knockout mice on C57/BL6

© 2010 WILEY-VCH Verlag GmbH & Co. KGaA, Weinheim

genetic background and their age and sex-matched wild-type littermates ($ASM^{+/+}$). The $ASM^{-/-}$ mice [14, 15] were a kind gift of Dr. Verena Jendrossek (University of Tübingen, Germany) and were originally obtained from Dr. R. Kolesnick (Sloan Kettering Cancer Memorial Center, NY, USA). DCs were cultured as described previously [16–18], with slight modifications. Briefly, bone marrow cells were flushed out of the cavities from the femur and tibia with PBS. Cells were washed twice with RPMI and seeded out at a density of 2×10^6 cells *per* 60 mm dish. Cells were cultured for 8 days in RPMI 1640 (GIBCO, Carlsbad) containing: 10% fetal calf serum (FCS), 1% penicillin/streptomycin, 1% glutamine, 1% nonessential amino acids and 0.05% β-mercaptoethanol. Cultures were supplemented with GM-CSF (35 ng/mL, Preprotech Tebu) and fed with fresh medium containing GM-CSF on days 3 and 6. Nonadherent and loosely adherent cells were harvested after 8 days of culture. At day 8, >80% of the cells expressed CD11c, which is a marker for mouse DCs. Experiments were performed in the absence or in the presence of different concentrations of thymol (2–100 μg/mL, Sigma-Aldrich, Taufkirchen, Germany) and in the absence and in the presence of amitriptyline (0.5 μM, Sigma-Aldrich) at day 9.

2.2 Ceramide formation detected by flow cytometry

For the detection of ceramide formation, mouse DCs were stained for 60 min at 37°C with anti-ceramide antibodies (Mouse IgM, Alexis) at a dilution of 1:10 in PBS containing 0.1% FCS [19]. After three washes with PBS/0.1% FCS, cells were stained with FITC–labeled goat anti-mouse IgG antibody at a dilution of 1:400 (Invitrogen, Germany) in PBS/0.1% FCS for 30 min at 37°C. Unbound secondary antibodies were removed by washing the cells with PBS/0.1% FCS. Cells were then analyzed by flow cytometry (FACS Calibur, BD Biosciences) (FACS, fluorescence-activated cell sorting).

2.3 Immunocytochemistry for ceramide formation

Untreated or thymol-treated (20 μg/mL, 24 h) DCs were smeared onto glass slides, rinsed in PBS and fixed with 4% formaldehyde in PBS for 15 min at room temperature. After three washing steps with PBS for 5 min, slides were permeabilized and blocked in PBS containing 5% goat serum (Invitrogen, Karlsruhe, Germany) and 0.3% Triton X-100 for 60 min and then incubated overnight at 4°C with anti-ceramide antibodies (Mouse IgM, Alexis) at a dilution of 1:10 in antibody dilution buffer (including PBS, 1% BSA and 0.3% Triton X-100). The slides were washed again three times for 5 min and then incubated with goat anti-mouse IgG-FITC (Invitrogen, Germany) in antibody dilution buffer for 90 min at 1:500 dilution at room temperature in dark. After three washing steps with PBS, nuclei were stained with DRAQ5 (1:1000, BioStatus, Shepshed, Leicestershire, UK) in PBS containing 0.5%Triton X-100 for 10 min and washed finally two times with PBS. Stained slides were mounted using Prolong® Gold antifade reagent (Invitrogen, Germany). Images were taken on a Zeiss LSM 5 EXCITER Confocal Laser Scanning Microscope (Carl Zeiss Micro-Imaging GmbH, Germany) with immersion Plan-Neofluar 10_/1.3 NA DIC objective and camera function.

2.4 ASM activity assay

The activity of the ASM was measured as described previously [20]. Briefly, 5×10^5cells were incubated with thymol (20 μg/mL) for different time spans: 30 min, 1 h, 5 h, 8 h or 24 h, frozen in liquid nitrogen and kept at −80°C. Then the cells were lysed in 50 μL of ice-cold buffer containing 50 mM sodium acetate (pH 5.0), 1% NP40. After 10 min lysis on ice, the lysates were diluted to 0.1% NP40 in a final volume of 200 μL. The lysates were incubated with 0.02 μCi of [^{14}C]sphingomyelin for 30 min at 37°C. The reaction was stopped by addition of 1 ml of $CHCl_3$:CH_3OH v/v. The substrate was dried before use and resuspended in 50 mM sodium acetate (pH 5.0), 0.2% Triton X-100, followed by 10 min bath sonication to promote the formation of micelles. Phases were separated by 5 min centrifugation at 14 000 rpm, and an aliquot of the aqueous phase was applied for liquid scintillation counting. Hydrolysis of [^{14}C]sphingomyelin by sphingomyelinase results in release of [^{14}C]choline chloride into the aqueous phase, whereas ceramide and unreacted [^{14}C]sphingomyelin remain in the organic phase. Therefore, the release of [^{14}C]choline chloride (pmol/10^5 cells/h) serves to determine the activity of the ASM.

2.5 Biochemical ceramide assay

Cellular ceramide levels were measured with a 1,2-diacylglycerol (DAG) kinase assay as described previously [21]. Briefly, 5×10^5 cells were incubated with thymol (20 μg/mL) for different time spans: 30 min, 1 h, 5 h, 8 h or 24 h, frozen in liquid nitrogen and kept at −80°C. Then the cells were lysed in 250 mM Na-acetate, 0.1% NP40, 1.3 mM EDTA and extracted in $CHCl_3$:CH_3OH:1 N HCl (100:100:1, v/v/v). Phases were separated, and the lower phase was collected, dried and subjected to alkaline hydrolysis of DAG in 0.1 N methanolic KOH at 37°C for 60 min. Samples were extracted again, and the lower phase was dried. Samples were resuspended in 20 μL detergent solution consisting of 7.5% w/v *n*-octyl glucopyranoside and 5 mM cardiolipin in 1 mM diethylenetriaminepentaacetic acid. Samples were then sonicated for 10 min in a bath sonicator; to these samples, 70 mL of an assay buffer was added consisting of 0.1 M imidazole/HCl (pH 6.6), 0.1 M NaCl, 25 mM $MgCl_2$ and 2 mM EGTA; 2.8 mM DTT; 5 μM ATP; 10 μCi of [^{32}P]ATP; 10 μL DAG

© 2010 WILEY-VCH Verlag GmbH & Co. KGaA, Weinheim

kinase (diluted in 1 mM diethylenetriaminepentaacetic acid; pH 6.6) and 0.01 M imidazole/HCl. The kinase reaction was performed for 30 min at room temperature, and the samples were extracted in 1 mL $CHCl_3$:CH_3OH:1 N HCl (100:100:1, v/v/v), 170 μL buffered saline solution (135 mM NaCl, 1.5 mM $CaCl_2$, 0.5 mM $MgCl_2$, 5.6 mM glucose, 10 mM HEPES; pH 7.2) and 30 μL 100 mM EDTA solution. Phases were separated and the lower phase was dried. Samples were dissolved in 20 mL $CHCl_3$:CH_3OH (1:1, v/v). Lipids were separated on Silica G-60 TLC plates with $CHCl_3$:Aceton:Methanol:Acetic-Acid:H_2O (60:24:18:12:6) and the plates were dried and exposed. Ceramide spots were identified by comigration with a C_{16}-ceramide standard and removed from the plate. The incorporation of [^{32}P] into ceramide was quantified by liquid scintillation counting. Comparison with a standard curve using C_{16}-ceramide permitted the determination of ceramide amounts.

2.6 DNA fragmentation

Briefly, 5×10^5 cells were fixed with 2% formaldehyde for 30 min on ice and then incubated with 70% ethanol for 15 min at 37°C. Cells were then treated with RNase A (40 μg/mL) for 30 min at 37°C, washed and resuspended in 200 μL propidium iodide (PI) (50 μg/mL, Sigma). DNA content of the samples was analyzed by flow cytometry (FACS Calibur, BD Biosciences).

2.7 Caspase 8 and caspase 3 activity assay

The activity of caspase 8 and caspase 3 was determined using kits from Biovision according to the manufacturer's instructions. Briefly, 1×10^6 cells were washed twice with cold PBS, fixed and permeabilized with ''Cytofix/Cytoperm'' solution and then by washing twice with ''Perm/Wash'' buffer. Then cells were stained with FITC-conjugated anti-active caspase 8 or caspase 3 antibody in ''Perm/Wash'' buffer for 60 min. After two washing steps, the cells were analyzed by flow cytometry (FACS Calibur, BD Biosciences).

2.8 Phosphatidylserine translocation

Apoptotic cell membrane scrambling was evidenced from annexin V binding to phosphatidylserine at the cell surface [22]. The percentage of phosphatidylserine-translocating cells was evaluated by staining with FITC-conjugated annexin V. In brief, 4×10^5 cells were harvested and washed twice with annexin washing buffer (AWB, 10 mM Hepes/NaOH, pH 7.4, 140 mM NaCl, 5 mM $CaCl_2$). The cell pellet was resuspended in 100 μL of Annexin-V-Fluos labeling solution (Roche) (20 μL Annexin-V-Fluos labeling reagent in 1 mL AWB), incubated for 15 min at room temperature. After washing with AWB, they were analyzed by flow cytometry.

2.9 Immunoblotting

DCs (2×10^6 cells) were washed twice in PBS and then solubilized in lysis buffer (Pierce) containing protease inhibitor cocktail (Sigma-Aldrich). Samples were stored at −80°C until use for Western blotting. Cell lysates were separated by 12% SDS-PAGE and blotted on nitrocellulose membranes. The blots were blocked with 5% nonfat-milk in triethanolamine-buffered saline and 0.1% Tween-20. Then the blots were probed overnight with monoclonal antibodies directed against either Bcl-2 or Bcl-xL (Santa Cruz) or α/β-tubulin (Cell Signaling) diluted (1:200 for Bcl-2 and Bcl-xL, or 1:1000 for α/β-tubulin) in blocking buffer, washed five times, probed with secondary antibodies (anti-mouse or anti-rabbit, GE Healthcare) diluted 1:5000 for 1 h at room temperature and washed finally five times. Antibody binding was detected with the enhanced chemiluminescence kit (Amersham, Freiburg, Germany). Densitometer scans of the blots were performed using Quantity One (BioRad, Munich, Germany).

2.10 Fas small interfering RNA

Fas-targeted small interfering RNA (siRNA) (RNA, Santa Cruz) was transfected into DCs (10^5 cells/1 mL) at a final concentration of 100 nM using Nucleofector technology (Amaxa) according to the manufacturer's recommendations. After electroporation, cells were incubated for 24 h at 37°C, 5% CO_2. After washing three times with PBS, the cells were incubated for 24 h with thymol (20 μg/mL).

2.11 Real-time PCR

Total RNA was isolated from mouse DCs by using the Qiashredder and RNeasy Mini Kit from Qiagen. For cDNA first strand synthesis, 1 μg of total RNA in 12.5 μL DEPC-H_2O was mixed with 1 μL of oligo-dT primer (500 μg/mL, Invitrogen) and heated for 2 min at 70°C. To determine Fas transcript levels, quantitative real-time PCR with the LightCycler System (Roche Diagnostics, Mannheim, Germany) was applied. The following primers were used: Fas primers (sc-29312-PR, Santa Cruz) and actin primers: 5′-CATTGCTGACAGGATGCAGAA-3′ (forward) and 5′-ATGGTGCTAGGAGCCAGAGC-3′ (reverse). PCR reactions were performed in a final volume of 20 μL containing 2 μL cDNA, 2.4 μL $MgCl_2$ (3 μM), 1 μL primer mix (0.5 μM of both primers), 2 μL cDNA Master SybrGreen I mix (Roche Molecular Biochemicals, Mannheim, Germany) and 12.6 μL DEPC-treated water. The target DNA was amplified during 40 cycles of 95°C for 10 s, 62°C for 10 s and 72°C for 16 s, each with a temperature transition rate of 20°C/s, a secondary target temperature of 50°C and a step size of 0.5°C. Melting curve analysis was performed at 95°C, 0 s; 60°C, 10 s and 95°C, 0 s to determine the melting

© 2010 WILEY-VCH Verlag GmbH & Co. KGaA, Weinheim

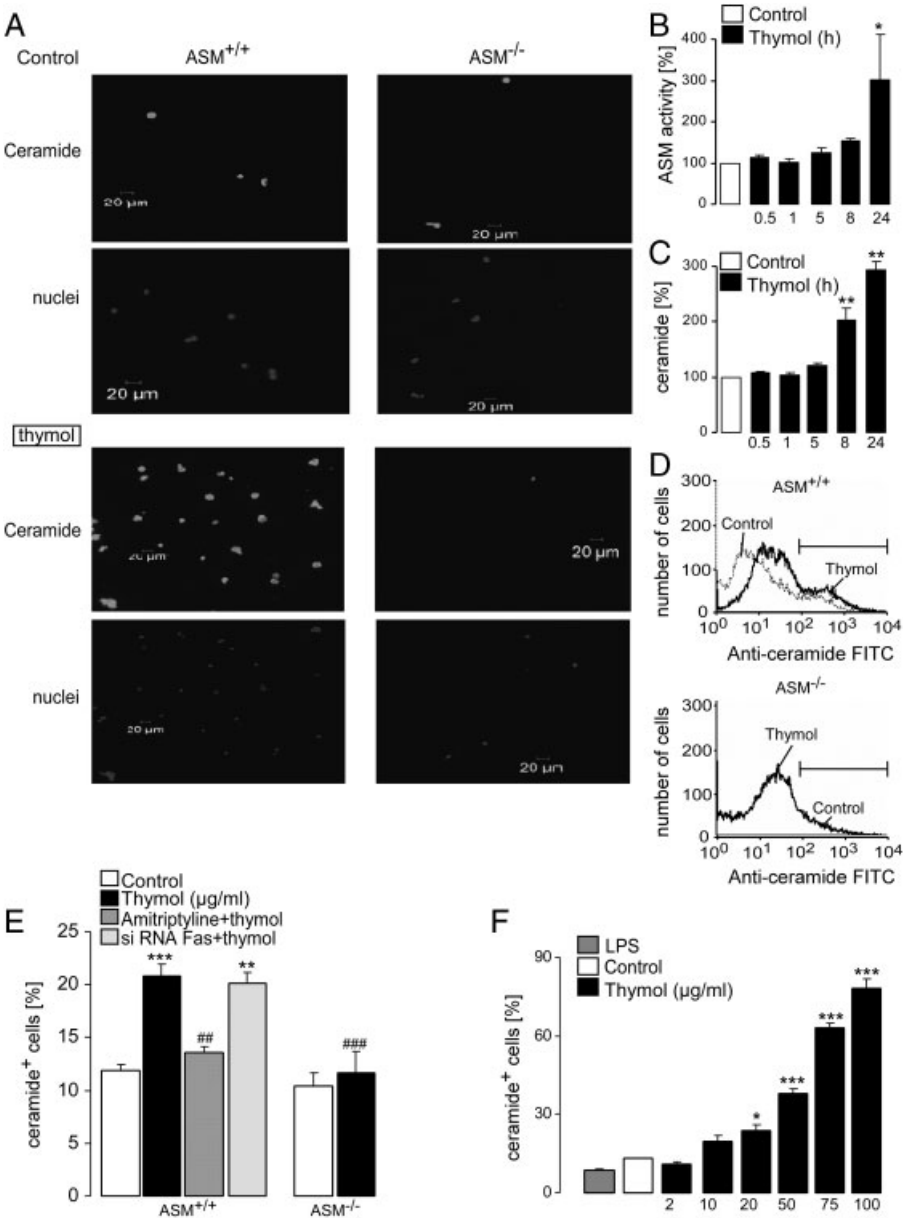

Figure 1. Effect of thymol on ceramide formation in DCs. (A) Immunohistochemistry of anti-ceramide FITC-coupled-antibody binding and nuclear staining in a representative experiment on wild-type (left panels) and ASM$^{-/-}$ DCs (right panels) either untreated (control, upper panels) or incubated for 24 h with thymol (20 μg/mL, lower panels). (B) Enzymatic activity of ASM in wild-type DCs treated with thymol for different time periods: 30 min, 1 h, 5 h, 8 h and 24 h as % to untreated cells ($n = 2$–3). $^{*}p < 0.05$, Dunnett multiple comparison test, ANOVA. (C) DAG kinase assays of total cellular ceramide contents in wild-type DCs treated with thymol for different time periods: 30 min, 1 h, 5 h, 8 h and 24 h in % of the respective value in untreated cells ($n = 2$–3). $^{**}p < 0.01$, Dunnett multiple comparison test, ANOVA. (D) Histograms of anti-ceramide FITC-coupled-antibody binding as obtained by FACS analysis in a representative experiment on wild-type (ASM$^{+/+}$, upper panel) and ASM$^{-/-}$ DCs (lower panel) either untreated (control, dotted line) or incubated for 24 h with thymol (20 μg/mL, black line). (E) Arithmetic means ($n = 4$–6) of the percentage of wild-type (ASM$^{+/+}$, left bars) and ASM$^{-/-}$ (right bars) DCs presenting ceramide at the cell surface. Ceramide formation is shown prior to (control, white bars) and 24 h following treatment with thymol (20 μg/mL) either in the absence (black bars) or, in wild-type cells, in the presence of amitriptyline (0.5 μM, dark grey bars) or in wild-type cells transfected with Fas siRNA (light grey bars). $^{**}p < 0.01$ and $^{***}p < 0.001$ represent significant difference from wild-type cells under control conditions and $^{\#\#}p < 0.01$ and $^{\#\#\#}p < 0.001$ represent significant difference from thymol-treated wild type, ANOVA. (F) Dose-dependent effect of thymol on ceramide formation. Arithmetic means ($n = 4$–6) of the percentage of wild-type DCs presenting ceramide at the cell surface. Ceramide formation is shown in untreated cells (control, white bars) or in DCs either treated with LPS (0.1 μg/mL, 24 h, dotted bars) or thymol (2–100 μg/mL, black bars) $^{*}p < 0.05$ and $^{***}p < 0.001$ represent significant difference from control condition, ANOVA.

© 2010 WILEY-VCH Verlag GmbH & Co. KGaA, Weinheim

temperature of primer dimers and the specific PCR products.

2.12 Statistics

Data are provided as means ± SEM, n represents the number of independent experiments. Differences were tested for significance using ANOVA. $p < 0.05$ was considered statistically significant.

3 Results

To determine the effect of thymol on murine bone marrow-derived DCs, the cells were grown in GM-CSF containing media for 8 days and subsequently exposed to thymol. In DCs stained with anti-ceramide antibodies, a marked accumulation of cellular ceramide was observed after treatment with 20 μg/mL thymol (24 h, Fig. 1A). No ceramide formation was observed in thymol-treated DCs from mice lacking functional $ASM^{-/-}$. The measurements of ASM enzymatic activity in wild-type DCs treated with thymol for different time periods indicated a strong ASM activation after 24 h of incubation with thymol (20 μg/mL, Fig. 1B). To confirm ceramide accumulation in thymol-treated DCs, we performed DAG kinase assays that determine total cellular ceramide concentrations. We detected a substantial increase in ceramide concentrations in DCs treated with thymol (20 μg/mL) for 8 and 24 h (Fig. 1C). Measurements of ceramide formation by flow cytometry confirmed that administration of thymol within 24 h stimulated ceramide formation in DCs from wild-type mice but not in DCs from $ASM^{-/-}$ mice (Figs. 1D and E) and not in wild-type cells treated with sphingomyelinase inhibitor amitriptyline (Fig. 1E). Accordingly, thymol stimulated the formation of ceramide by activation of the ASM. For statistically significant effects on ceramide production, 20 μg/mL thymol was required (Fig. 1F). DC activation by LPSs *via* Toll-like receptor 4 ligation is known to inhibit DC apoptosis [9]. Addition of LPS to DCs tended to slightly downregulate ceramide formation, an effect, however, not reaching statistical significance (Fig. 1E and also Figs. 2–5C). Ceramide formation was not dependent on Fas (CD95), since treatment of DCs with siRNA for Fas (CD95) did not prevent thymol-induced ceramide formation in wild-type DCs (Fig. 1E).

The stimulation of ceramide formation by thymol was followed by activation of caspase 8 and caspase 3 (Figs. 2 and 3), an effect reaching statistical significance at the concentration of 50 μg/mL (Figs. 2C and 3C). Thymol stimulated caspase 8 and caspase 3 only in wild-type DCs but not in DCs derived from $ASM^{-/-}$ mice (Figs. 2A and B and Figs. 3A and B) or in wild-type DCs treated with amitriptyline (Figs. 2B and 3B), demonstrating that the stimulation of caspases by thymol required the activation of ASM.

The activation of caspases was expected to trigger DC apoptosis. Thus, further experiments have been performed to elucidate, whether thymol trigered DNA fragmentation, one of the hallmarks of apoptosis. The exposure to thymol at concentrations ≥10 μg/mL was indeed followed by an

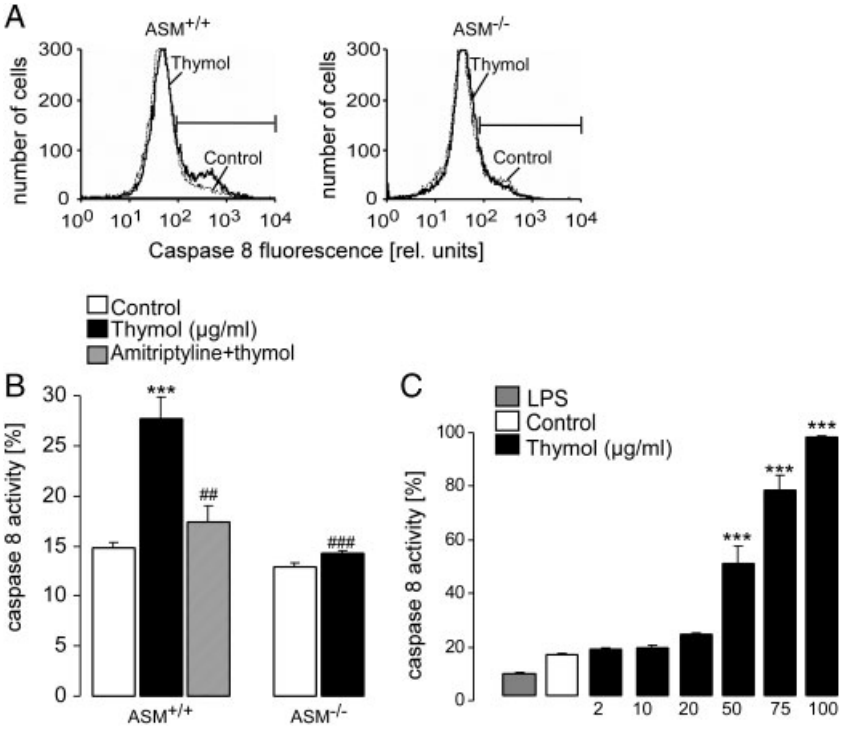

Figure 2. Effect of thymol on caspase 8 activity in DCs. (A) Histograms of caspase 8 activity as obtained by FACS analysis in a representative experiment on wild-type and $ASM^{-/-}$ DCs either untreated (control, dotted line) or incubated for 24 h with thymol (20 μg/mL, black line). (B) Arithmetic means ($n = 4$–6) of the percentage of wild-type ($ASM^{+/+}$, left bars) and $ASM^{-/-}$ (right bars) DCs with activated caspase 8. Caspase activation is shown prior to (control, white bars) and 24 h following treatment with thymol (20 μg/mL) either in the absence (black bars) or, also in wild type cells, in the presence of amitriptyline (0.5 μM, hatched bars). $^{***}p < 0.001$ represents significant difference from wild-type cells under control conditions; $^{\#\#}p < 0.01$ and $^{\#\#\#}p < 0.001$ represent significant difference from thymol-treated wild-type DCs, ANOVA. (C) Dose-dependent effect of thymol on caspase 8 activation. Arithmetic means ($n = 4$–6) of the percentage of wild-type DCs with activated caspase 8. Caspase 8 activity is shown in untreated cells (control, white bars) or in DCs either treated with LPS (0.1 μg/mL, 24 h, dotted bars) or thymol (2–100 μg/mL, black bars). $^{***}p < 0.001$ represents significant difference from control condition, ANOVA.

© 2010 WILEY-VCH Verlag GmbH & Co. KGaA, Weinheim

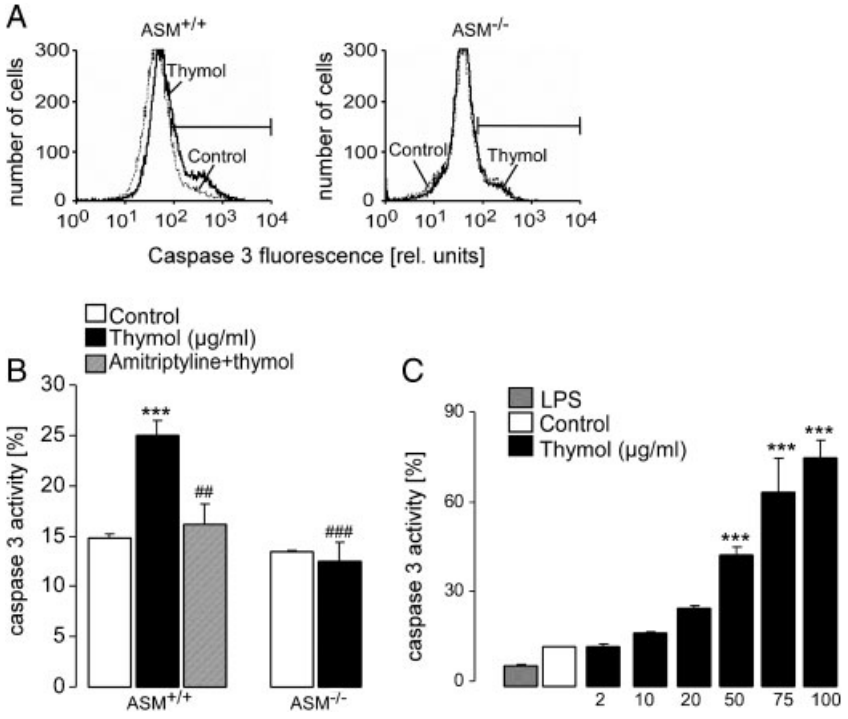

Figure 3. Effect of thymol on caspase 3 activity in DCs. (A) Histograms of caspase 3 activity as obtained by FACS analysis in a representative experiment on wild-type and ASM$^{-/-}$ DCs either untreated (control, dotted line) or incubated for 24 h with thymol (20 μg/mL, black line). (B) Arithmetic means ($n = 4$–6) of the percentage of wild-type (ASM$^{+/+}$, left bars) and ASM$^{-/-}$ (right bars) DCs with activated caspase 3. Caspase activation is shown prior to (control, white bars) and 24 h following treatment with thymol (20 μg/mL) either in the absence (black bars) or, also in wild-type cells, in the presence of amitriptyline (0.5 μM, hatched bars). $^{***}p<0.001$ represents significant difference from wild-type cells under control conditions; $^{\#\#}p<0.01$ and $^{\#\#\#}p<0.001$ represent significant difference from thymol-treated wild-type DCs, ANOVA. (C) Dose-dependent effect of thymol on caspase 3 activation. Arithmetic means ($n = 4$–6) of the percentage of wild-type DCs with activated caspase 3. Caspase 3 activity is shown in untreated cells (control, white bars) or in DCs either treated with LPS (0.1 μg/mL, 24 h, dotted bars) or treated with thymol (2–100 μg/mL, black bars).$^{***}p<0.001$ represents significant difference from control condition, ANOVA.

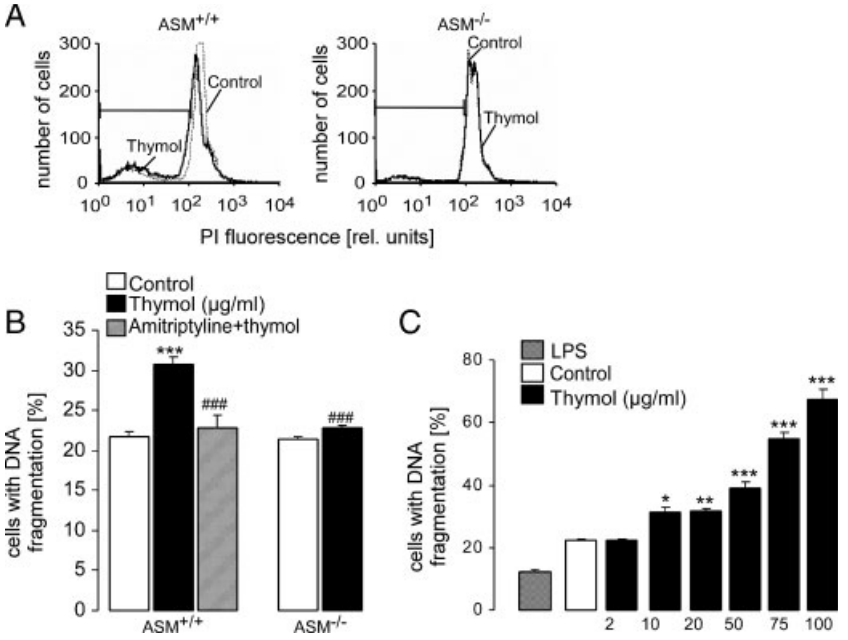

Figure 4. Effect of thymol on DNA fragmentation in DCs. (A) Histograms of PI fluorescence as obtained by FACS analysis in a representative experiment on wild-type and ASM$^{-/-}$ DCs either untreated (control, dotted line) or incubated for 24 h with thymol (20 μg/mL, black line). (B) Arithmetic means ($n = 4$–6) of the percentage of wild-type (ASM$^{+/+}$, left bars) and ASM$^{-/-}$ (right bars) DCs with fragmented DNA. DNA fragmentation is shown prior to (control, white bars) and 24 h following treatment with thymol (20 μg/mL) either in the absence (black bars) or, also in wild-type cells, in the presence of amitriptyline (0.5 μM, hatched bars). $^{***}p<0.001$ represents significant difference from wild-type cells under control conditions and $^{\#\#\#}p<0.001$ represents significant difference from thymol-treated wild-type DCs, ANOVA. (C) Dose-dependent effect of thymol on DNA fragmentation. Arithmetic means ($n = 4$–6) of the percentage of wild-type DCs with fragmented DNA. DNA fragmentation is shown in untreated cells (control, white bars) or in DCs either treated with LPS (0.1 μg/mL, 24 h, dotted bars) or treated with thymol (2–100 μg/mL, black bars). $^{*}p<0.05$, $^{**}p<0.01$ and $^{***}p<0.001$ represent significant difference from control condition, ANOVA.

© 2010 WILEY-VCH Verlag GmbH & Co. KGaA, Weinheim

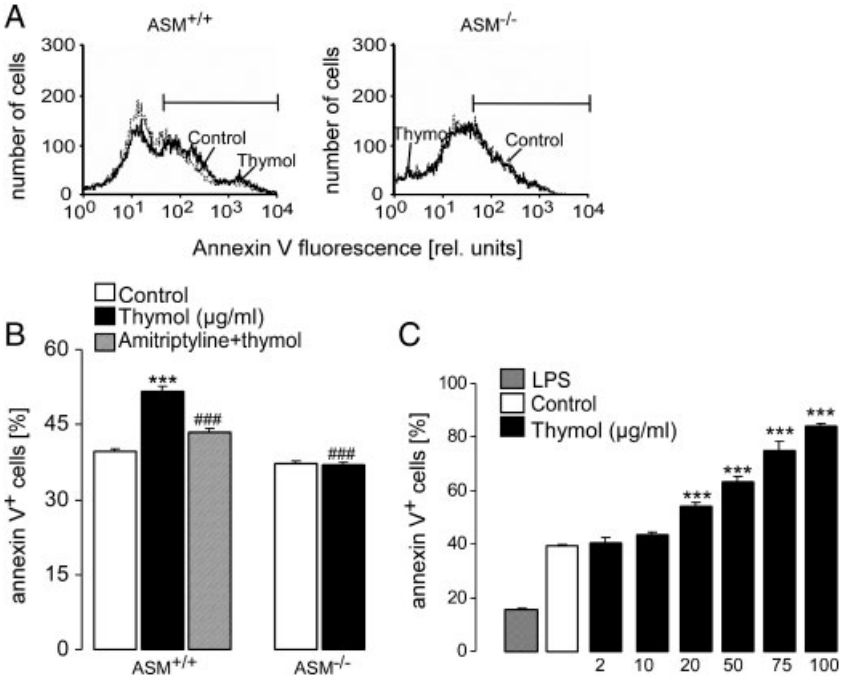

Figure 5. Effect of thymol on cell membrane scrambling in DCs. (A) Histograms of annexin V binding as obtained by FACS analysis in a representative experiment on wild-type and ASM$^{-/-}$ DCs either untreated (control, dotted line) or incubated for 24 h with thymol (20 μg/mL, black line). (B) Arithmetic means ($n = 4$–6) of the percentage of wild-type (ASM$^{+/+}$, left bars) and ASM$^{-/-}$ (right bars) DCs with annexin V binding. Annexin V binding is shown prior to (control, white bars) and 24 h following treatment with thymol (20 μg/mL) either in the absence (black bars) or, also in wild type cells, in the presence of amitriptyline (0.5 μM, hatched bars). $^{***}p < 0.001$ represents significant difference from wild-type cells under control conditions and $^{\#\#\#}p < 0.001$ represents significant difference from thymol-treated wild-type DCs, ANOVA. (C) Dose-dependent effect of thymol on annexin V binding. Arithmetic means ($n = 4$–6) of the percentage of wild-type DCs with annexin V binding are shown in untreated cells (control, white bars) or in DCs either treated with LPS (0.1 μg/mL, 24 h, dotted bars) or treated with thymol (2–100 μg/mL, black bars). $^{***}p < 0.001$ represents significant difference from control condition, ANOVA.

increase of cells in the sub-G1 phase, a marker for fragmented DNA (Fig. 4). On the contrary, thymol did not elicit DNA fragmentation in DCs derived from ASM$^{-/-}$ mice or in wild-type DCs treated with amitriptyline.

Another hallmark of apoptosis is cell membrane scrambling leading to phosphatidylserine exposure at the cell surface. The phosphatidylserine exposure was determined from annexin V binding. As shown in Fig. 5, exposure of DCs to thymol at concentrations above 20 μg/mL was followed by stimulation of annexin V binding in wild type but not in ASM$^{-/-}$ DCs and not when wild-type DCs were treated with amitriptyline.

Moreover, thymol treatment resulted in reduction of the abundance of anti-apoptotic Bcl-2 and Bcl-xL proteins in wild-type DCs (Fig. 6). Downregulation of Bcl-2 and Bcl-xL proteins by thymol was not observed in ASM$^{-/-}$ DCs (Fig. 6).

4 Discussion

This study reveals that thymol stimulates the ASM in DCs with subsequent formation of ceramide, downregulation of Bcl-2 and Bcl-xL protein expression, caspase activation and finally triggering of suicidal cell death.

Thymol has been administrated to animals at dosages of 100–150 mg/kg body weight and thus the concentrations employed here (20 μg/mL) could well be achieved in the intestinal lumen [23, 24], which is in contact to intestinal DCs [13].

The sequence of events in thymol-induced apoptosis could be the following: DC stimulation with thymol leads to translocation of ASM from an intracellular compartment onto the cell surface. In lymphocytes, electron microscopy studies localized ASM in intracellular vesicles of unstimulated cells, which appeared to fuse with the cell membrane upon stimulation with the Fas ligand [25]. This resulted in exposure of the ASM on the extracellular membrane leaflet and subsequent formation of ceramide. In this study, thymol-induced ceramide production was not dependent on Fas. Ceramide formation results in caspase 8 autocatalysis that initiates apoptosis induction. Caspase 8 can then directly activate caspase 3. The activation of caspase 3 executes apoptosis by triggering DNA fragmentation and proteolysis of intracellular proteins.

© 2010 WILEY-VCH Verlag GmbH & Co. KGaA, Weinheim

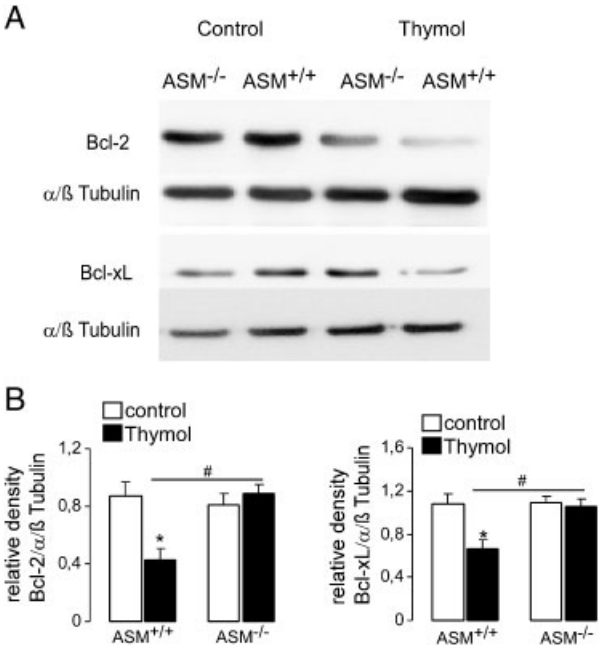

Figure 6. Effect of thymol on Bcl-2 and Bcl-xL protein abundance in wild-type and ASM$^{-/-}$ DCs. (A) Original Western blot of DCs from wild-type and ASM$^{-/-}$ mice, which were either treated with thymol (20 μg/mL, 24 h) or left untreated (control). Protein extracts were analyzed by direct Western blotting using antibodies directed to Bcl-2 or to Bcl-xL. Protein loading was controlled by anti-α/β-tubulin antibody. One representative experiment out of three is shown. (B, C) Arithmetic mean ± SEM ($n = 3$) of the abundance of Bcl-2 (B) or Bcl-xL (C) as the ratio of Bcl-2:α/β-tubulin or Bcl-xL:α/β-tubulin. $^{*}p < 0.05$ indicates significant difference between control and thymol-treated cells, $^{\#}p < 0.05$ indicates difference between thymol-treated wild-type and ASM$^{-/-}$ DCs, ANOVA.

To the best of our knowledge, an effect of thymol on sphingomyelinase or on ceramide formation has never been shown before. Thymol has been shown to exert some antioxidant activity [5] and to decrease the cytosolic Ca^{2+} activity [26]. Both effects would not be expected to induce cell death. On the contrary, stimulation of sphingomyelinase and subsequent formation of ceramide are well known to induce apoptosis [27–29].

The observation that thymol stimulates caspases and suicidal cell death or apoptosis is similarly novel. In erythrocytes, thymol even protects against suicidal cell death [7], which is triggered by stimulation of sphingomyelinase and subsequent formation of ceramide [22, 27, 30–32]. The present observations do not disclose the mechanisms underlying opposite effects of thymol on cell survival of erythrocytes and DCs. Clearly, the regulation of ceramide formation is distinct in DCs and erythrocytes. Moreover, the signaling of suicidal death is different between erythrocytes and nucleated cells, as erythrocytes lack mitochondria and nuclei, key players in apoptosis [27].

The thymol-induced apoptosis is expected to weaken the immune response, an effect which, at least in theory, may limit its use in the treatment of infectious disease. However, the effect on pathogens may be more pronounced and thymol may thus favourably influence the course of infectious disease [1, 2]. Nevertheless, the present observations provide a caveat on the use of thymol in infectious disease. On the other hand, the thymol-induced apoptosis may exert some anti-inflammatory action. In any case, the stimulation of ceramide formation and apoptotic death of DCs by thymol is expected to affect the immune response.

This work was supported by the Deutsche Forschungsgemeinschaft (SFB 766) and GU 335-13/3.

The authors have declared no conflict of interest.

5 References

[1] Burt, S., Essential oils: their antibacterial properties and potential applications in foods – a review. *Int. J. Food Microbiol.* 2004, *94*, 223–253.

[2] Razzaghi-Abyaneh, M., Shams-Ghahfarokhi, M., Yoshinari, T., Rezaee, M. B. *et al.*, Inhibitory effects of *Satureja hortensis* L. essential oil on growth and aflatoxin production by *Aspergillus parasiticus*. *Int. J. Food Microbiol.* 2008, *123*, 228–233.

[3] Guo, N., Liu, J., Wu, X., Bi, X. *et al.*, Antifungal activity of thymol against clinical isolates of fluconazole-sensitive and -resistant *Candida albicans*. *J. Med. Microbiol.* 2009, *58*, 1074–1079.

[4] Kim, D. O., Lee, C. Y., Comprehensive study on vitamin C equivalent antioxidant capacity (VCEAC) of various polyphenolics in scavenging a free radical and its structural relationship. *Crit. Rev. Food Sci. Nutr.* 2004, *44*, 253–273.

[5] Undeger, U., Basaran, A., Degen, G. H., Basaran, N., Antioxidant activities of major thyme ingredients and lack of (oxidative) DNA damage in V79 Chinese hamster lung fibroblast cells at low levels of carvacrol and thymol. *Food Chem. Toxicol.* 2009, *47*, 2037–2043.

[6] Stammati, A., Bonsi, P., Zucco, F., Moezelaar, R. *et al.*, Toxicity of selected plant volatiles in microbial and mammalian short-term assays. *Food Chem. Toxicol.* 1999, *37*, 813–823.

[7] Mahmud, H., Mauro, D., Föller, M., Lang, F., Inhibitory effect of thymol on suicidal erythrocyte death. *Cell. Physiol. Biochem.* 2009, *24*, 407–414.

[8] Adler, H. S., Steinbrink, K., Tolerogenic dendritic cells in health and disease: friend and foe! *Eur. J. Dermatol.* 2007, *17*, 476–491.

[9] Banchereau, J., Briere, F., Caux, C., Davoust, J. *et al.*, Immunobiology of dendritic cells. *Annu. Rev. Immunol.* 2000, *18*, 767–811.

[10] van Duivenvoorde, L. M., Han, W. G., Bakker, A. M., Louis-Plence, P. *et al.*, Immunomodulatory dendritic cells inhibit

© 2010 WILEY-VCH Verlag GmbH & Co. KGaA, Weinheim

Th1 responses and arthritis via different mechanisms. *J. Immunol.* 2007, *179*, 1506–1515.

[11] Cerovic, V., McDonald, V., Nassar, M. A., Paulin, S. M. *et al.*, New insights into the roles of dendritic cells in intestinal immunity and tolerance. *Int. Rev. Cell. Mol. Biol.* 2009, *272*, 33–105.

[12] Rescigno, M., Lopatin, U., Chieppa, M., Interactions among dendritic cells, macrophages, and epithelial cells in the gut: implications for immune tolerance. *Curr. Opin. Immunol.* 2008, *20*, 669–675.

[13] Chieppa, M., Rescigno, M., Huang, A. Y., Germain, R. N., Dynamic imaging of dendritic cell extension into the small bowel lumen in response to epithelial cell TLR engagement. *J. Exp. Med.* 2006, *203*, 2841–2852.

[14] Horinouchi, K., Erlich, S., Perl, D. P., Ferlinz, K. *et al.*, Acid sphingomyelinase deficient mice: a model of types A and B Niemann-Pick disease. *Nat. Genet.* 1995, *10*, 288–293.

[15] Lin, T., Genestier, L., Pinkoski, M. J., Castro, A. *et al.*, Role of acidic sphingomyelinase in Fas/CD95-mediated cell death. *J. Biol. Chem.* 2000, *275*, 8657–8663.

[16] Inaba, K., Inaba, M., Romani, N., Aya, H. *et al.*, Generation of large numbers of dendritic cells from mouse bone marrow cultures supplemented with granulocyte/macrophage colony-stimulating factor. *J. Exp. Med.* 1992, *176*, 1693–1702.

[17] Shumilina, E., Zahir, N., Xuan, N. T., Lang, F., Phosphoinositide 3-kinase dependent regulation of Kv channels in dendritic cells. *Cell. Physiol. Biochem.* 2007, *20*, 801–808.

[18] Matzner, N., Zemtsova, I. M., Nguyen Thi, X., Duszenko, M., Shumilina, E., Lang, F., Ion channels modulating mouse dendritic cell functions. *J. Immunol.* 2008, *181*, 6803–6809.

[19] Lang, K. S., Myssina, S., Brand, V., Sandu, C. *et al.*, Involvement of ceramide in hyperosmotic shock-induced death of erythrocytes. *Cell. Death Differ.* 2004, *11*, 231–243.

[20] Grassme, H., Jendrossek, V., Riehle, A., von Kurthy, G. *et al.*, Host defense against *Pseudomonas aeruginosa* requires ceramide-rich membrane rafts. *Nat. Med.* 2003, *9*, 322–330.

[21] Zhang, Y., Li, X., Carpinteiro, A., Gulbins, E., Acid sphingomyelinase amplifies redox signaling in *Pseudomonas aeruginosa*-induced macrophage apoptosis. *J. Immunol.* 2008, *181*, 4247–4254.

[22] Wang, K., Mahmud, H., Foller, M., Biswas, R. *et al.*, Lipopeptides in the triggering of erythrocyte cell membrane scrambling. *Cell. Physiol. Biochem.* 2008, *22*, 381–386.

[23] Azirak, S., Rencuzogullari, E., The *in vivo* genotoxic effects of carvacrol and thymol in rat bone marrow cells. *Environ. Toxicol.* 2008, *23*, 728–735.

[24] Luna, A., Labaque, M. C., Zygadlo, J. A., Marin, R. H., Effects of thymol and carvacrol feed supplementation on lipid oxidation in broiler meat. *Poult. Sci.* 2010, *89*, 366–370.

[25] Grassme, H., Schwarz, H., Gulbins, E., Molecular mechanisms of ceramide-mediated CD95 clustering. *Biochem. Biophys. Res. Commun.* 2001, *284*, 1016–1030.

[26] Suzuki, Y., Nakamura, S., Sugiyama, K., Furuta, H., Differences of superoxide production in blood leukocytes stimulated with thymol between human and non-human primates. *Life Sci.* 1987, *41*, 1659–1664.

[27] Lang, F., Gulbins, E., Lerche, H., Huber, S. M. *et al.*, Eryptosis, a window to systemic disease. *Cell. Physiol. Biochem.* 2008, *22*, 373–380.

[28] Perrotta, C., De Palma, C., Clementi, E., Nitric oxide and sphingolipids: mechanisms of interaction and role in cellular pathophysiology. *Biol. Chem.* 2008, *389*, 1391–1397.

[29] Smith, E. L., Schuchman, E. H., The unexpected role of acid sphingomyelinase in cell death and the pathophysiology of common diseases. *FASEB J.* 2008, *22*, 3419–3431.

[30] Brand, V., Koka, S., Lang, C., Jendrossek, V. *et al.*, Influence of amitriptyline on eryptosis, parasitemia and survival of *Plasmodium berghei*-infected mice. *Cell. Physiol. Biochem.* 2008, *22*, 405–412.

[31] Sopjani, M., Foller, M., Dreischer, P., Lang, F., Stimulation of eryptosis by cadmium ions. *Cell. Physiol. Biochem.* 2008, *22*, 245–252.

[32] Sopjani, M., Foller, M., Gulbins, E., Lang, F., Suicidal death of erythrocytes due to selenium-compounds. *Cell. Physiol. Biochem.* 2008, *22*, 387–394.

© 2010 WILEY-VCH Verlag GmbH & Co. KGaA, Weinheim